

# Naturally Occurring Sphalerite As a Novel Cost-Effective Photocatalyst for Bacterial Disinfection under Visible Light

Yanmin Chen,<sup>†</sup> Anhuai Lu,<sup>‡</sup> Yan Li,<sup>‡</sup> Lisha Zhang,<sup>†</sup> Ho Yin Yip,<sup>†</sup> Huijun Zhao,<sup>§</sup> Taicheng An,<sup>‡</sup> and Po-Keung Wong<sup>\*,†</sup>

<sup>†</sup>School of Life Sciences, The Chinese University of Hong Kong, Shatin, NT, Hong Kong SAR, China

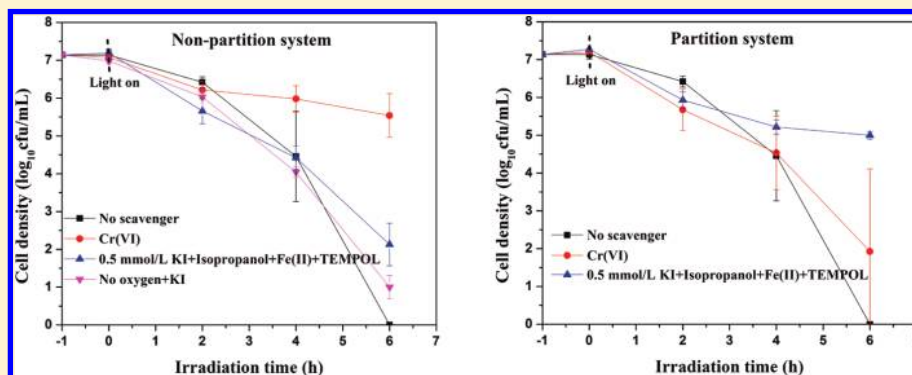
<sup>‡</sup>The Key Laboratory of Orogenic Belts and Crustal Evolution, School of Earth and Space Sciences, Peking University, Beijing 100871, China

<sup>§</sup>Centre for Clean Environment and Energy, and Griffith School of Environment, Gold Coast Campus, Griffith University, Queensland 4222, Australia

<sup>‡</sup>State Key Laboratory of Organic Geochemistry, Guangzhou Institute of Geochemistry, Chinese Academy of Sciences, Guangzhou 510640, China

 Supporting Information

## ABSTRACT:



The photocatalytic disinfection capability of the natural semiconducting mineral sphalerite is studied here for the first time. Natural sphalerite can completely inactivate  $1.5 \times 10^7$  cfu/mL *E. coli* K-12 within 6 h under visible light irradiation. The photocatalytic disinfection mechanism of natural sphalerite is investigated using multiple scavengers. The critical role that electrons play in bactericidal actions is experimentally demonstrated. The involvement of  $H_2O_2$  in photocatalytic disinfection is also confirmed using a partition system combined with different scavengers. Moreover, the photocatalytic destruction of bacterial cells is observed through transmission electron microscopic analysis. A catalase activity study reveals that antioxidative enzyme activity is high in the initial stage of photocatalytic disinfection but decreases with time due to damage to enzymatic functioning. Natural sphalerite is abundant and easy to obtain and possesses excellent visible-light photocatalytic activity. These superior properties make it a promising solar-driven photocatalyst for large-scale cost-effective wastewater treatment.

## 1. INTRODUCTION

Photocatalysis is a photoinduced advanced redox process based on the generation of powerful reactive species, such as the hydroxyl radical ( $\cdot OH$ ), hydrogen peroxide ( $H_2O_2$ ), the superoxide radical ( $\cdot O_2^-$ ), electrons ( $e^-$ ), and holes ( $h^+$ ).<sup>1</sup> The successful inactivation of *E. coli* by photocatalytic disinfection was first reported in 1985.<sup>2</sup> Since then, photocatalysis has been extensively studied and has proved to be a cost-effective, safe, and promising alternative for wastewater disinfection.

At present,  $TiO_2$ , which is a widely available commercial photocatalyst, is commonly used to degrade organic pollutants and disinfect bacteria.<sup>3,4</sup> However, with a bandgap of 3.2 eV,  $TiO_2$  can only be excited by UV, and thus much effort has been

devoted to synthesizing new visible-light-driven (VLD) photocatalysts. Although synthetic photocatalysts show promising disinfection performance under visible light (VL), the massive production of such synthetic photocatalysts at low cost has been a major limitation to its large-scale application. In this study, we introduce the natural photocatalyst sphalerite, which possesses VL photocatalytic activity and can be readily supplied in large quantities at low cost. It is envisaged that developing a natural

**Received:** October 13, 2010

**Accepted:** May 31, 2011

**Revised:** May 23, 2011

**Published:** June 14, 2011

photocatalyst-based disinfection technique will be an economically viable solution for large-scale practical wastewater treatment.

Natural sphalerite collected from the Huangshaping deposit was successfully applied to reduce heavy metal ions and reductively degrade azo dyes under VL.<sup>5–8</sup> Reports show that 91.95% of Cr<sup>6+</sup> and 98.74% of Methyl Orange can be photocatalytically reduced or decolorized within 9 and 2 h VL of irradiation, respectively. The effect of the conduction band e<sup>-</sup> on the reduction of heavy metal ions and the degradation of azo dyes were also reported in these studies.<sup>6,8</sup> More recently, it has been found that several active species, such as h<sup>+</sup>, •O<sub>2</sub><sup>-</sup>, H<sub>2</sub>O<sub>2</sub>, and •OH generated from the TiO<sub>2</sub>–UV system, can kill or inactivate bacteria. However, to date, no study has investigated the photocatalytic disinfection of bacteria by natural sphalerite under VL irradiation or reported whether e<sup>-</sup> can deactivate bacteria.

To study the bactericidal effect of natural sphalerite, a set of parallel experiments was designed to investigate (1) whether photocatalytic reaction occurs on the surface of photocatalysts, and (2) which reactive specie is the bactericidal agent in VLD photocatalytic disinfection. The suggested mechanism and reactive species involved in the photocatalytic disinfection of *E. coli* K-12 by natural sphalerite under VL irradiation are also discussed.

## 2. EXPERIMENTAL SECTION

**2.1. Materials.** The natural sphalerite used in this work was collected from the Huangshaping (HSP) deposit in Hunan Province, China.<sup>7</sup> The natural sphalerite sample was mechanically crushed and milled at the mine. The resultant sphalerite particles were passed through a 340-mesh sieve pore to obtain sphalerite powder with particle sizes <40 μm. The crystal structure of natural sphalerite was cubic, with a calculated lattice constant of  $a = 0.54264$  nm. The bandgap energy of natural sphalerite was 2.95 eV.<sup>7</sup>

**2.2. Photocatalytic Disinfection of *E. coli* K-12 in a Nonpartition System.** *Escherichia coli* K-12 (*E. coli* K-12) was chosen as the model bacterium because it was safe to use and easy to grow. A fluorescent tube (15 W, VELOX, Thailand) was selected as the VL source in the indoor premises used in this study. The bacterial cells were cultured in nutrient broth (BioLife, Milano, Italy) solution at 37 °C for 16 h with shaking and then washed with sterilized saline. The cell concentration was adjusted to a final cell density of  $1.5 \times 10^7$  cfu (colony forming unit)/mL in the reaction mixture.

Five mL of saline-washed *E. coli* K-12 was suspended in 45 mL sterilized saline (0.9% NaCl) solution containing the natural sphalerite. The reaction temperature was kept at 25 °C and the reaction mixture was stirred with a magnetic stirrer throughout the experiment. The reactor (Figure S1 of the Supporting Information) held six fluorescent tubes. The VL and UV intensities inside the reactor flask were measured by a light meter (LI-COR, Lincoln, Nebraska, USA) and an UVX digital radiometer (UVP, Upland, California, USA), respectively. A liquid filter (5 mol/L sodium nitrite) was placed between the fluorescent tubes and the sample flask to block all UV emission to determine whether natural sphalerite was a real VLD photocatalyst. The optimal concentration of the photocatalyst was 1.00 g/L (Figure S2 of the Supporting Information). At different time intervals, aliquots of the sample were collected and serially diluted with sterilized saline solution. Then, 0.1 mL of the diluted sample was immediately spread on nutrient agar plate

(Lancashire, UK) and incubated at 37 °C for 24 h to determine the number of viable cells (in cfu/mL). As a comparison, a dark control (natural sphalerite alone without light irradiation), a light control (light irradiation alone without the photocatalyst), and a negative control (without the natural sphalerite photocatalyst or light irradiation) were also conducted. Each set of experiments was performed in triplicate.

**2.3. Partition System.** To study whether direct contact between natural sphalerite and *E. coli* K-12 is important for disinfection, a partition system<sup>9–11</sup> was used to separate *E. coli* K-12 from the surface of natural sphalerite. The setup of the partition system for this experiment was shown in Figure S3 of the Supporting Information. Ten mL of *E. coli* K-12 suspension ( $1.5 \times 10^7$  cfu/mL) was pipetted into a semipermeable container, and 50 mL of the natural sphalerite suspension (1.00 g/L) was maintained outside of the membrane and stirred continuously to keep the natural sphalerite evenly distributed in the solution. At different intervals, aliquots of the cells inside the membrane were sampled and immediately diluted. The number of viable cells in the samples was determined by the same procedure as that described in Section 2.2.

**2.4. Effect of Scavengers.** The scavenger experiments were carried out by adding individual scavenger to nonpartition system and outside of the membrane container in partition system. KI was used to remove h<sup>+</sup> and •OH bound to the surface (•OHs),<sup>12</sup> isopropanol to remove •OH diffusing into the solution bulk,<sup>12,13</sup> 4-hydroxy-2,2,6,6-tetramethylpiperidinyloxy (TEMPOL) to remove •O<sub>2</sub><sup>-</sup>,<sup>14</sup> Cr(VI) to remove e<sup>-</sup>,<sup>12</sup> and Fe(II) to remove H<sub>2</sub>O<sub>2</sub>.<sup>11</sup>

When KI was added into the suspension, the concentration of I<sub>2</sub> produced in the photocatalytic disinfection system was detected by iodine-starch assay. At different time intervals, aliquots of the sample were collected, filtered through a Millipore filter (pore size of 0.45 μm), titrated with a starch solution, and measured the absorption at 540 nm by a UV–vis spectrophotometer.

**2.5. Transmission Electron Microscopy.** The mixture comprising the natural sphalerite and *E. coli* K-12 before and after the photocatalytic reaction was collected and centrifuged. The bacterial cells were prefixed by glutaraldehyde and trapped in low melting point agarose. After being postfixured by osmium tetroxide (E.M. grade, Electron Microscopy Sciences, Fort Washington, PA, USA), the cell pellet was dehydrated by adding a graded series of ethanol concentrations and was finally embedded in Spurr solution (Electron Microscopy Sciences, Fort Washington, PA, USA) for polymerization. Using an ultramicrotome (Leica, Reichert Ultracuts, Wien, Austria), ultrathin sections of 70 nm were made and stained with uranyl acetate and lead citrate on copper grids. Finally, the stained ultrathin sections were examined by a JEM-1200 EXII transmission electron microscope (JEOL Ltd., Tokyo, Japan).

**2.6. Measurement of Bacterial Catalase Activity and H<sub>2</sub>O<sub>2</sub>.** Catalase (CAT) activity was determined using a Catalase Assay Kit (Cayman Chemical Company, Ann Arbor, MI, USA) following the protocol in the instruction manual.<sup>15</sup> Hydrogen peroxide was analyzed photometrically by using the DPD/peroxidase method.<sup>16</sup>

## 3. RESULTS AND DISCUSSION

**3.1. Photocatalytic Disinfection Performance.** Figure 1 shows the photocatalytic disinfection of *E. coli* K-12 by natural sphalerite under VL irradiation. The bacterial population

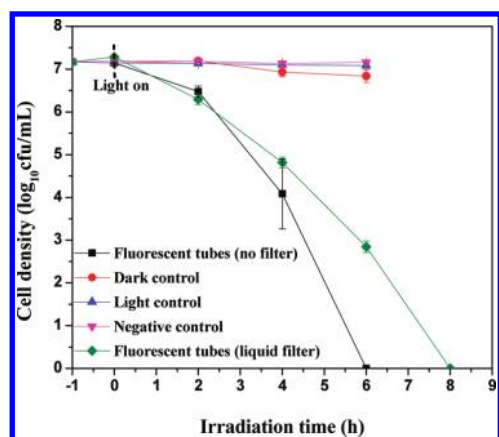


**Figure 1.** Photocatalytic disinfection of *E. coli* K-12 by the natural sphalerite under VL irradiation (without and with liquid filter). Experimental conditions: Fluorescent tubes without filter (visible light intensity = 3.3 mW/cm<sup>2</sup>, UVA intensity = 0.03 mW/cm<sup>2</sup>, UVB intensity = 0.015 mW/cm<sup>2</sup> and UVC intensity = 0.006 mW/cm<sup>2</sup>); fluorescent tubes with liquid filter (visible light intensity = 2.7 mW/cm<sup>2</sup>, no UVA, UVB, and UVC).

remained essentially unchanged after 6 h in all of the control experiments (Figure 1) suggesting that natural sphalerite has no toxic effect on bacterial cells and VL irradiation causes no photolysis in *E. coli* K-12. When the natural sphalerite was irradiated by VL, the bacterial population decreased with time until complete inactivation of *E. coli* K-12 was observed after 6 h of treatment (Figure 1).

Because the fluorescent tubes emit not only VL ( $\lambda \geq 400$  nm, the intensity = 3.3 mW/cm<sup>2</sup>) but also trace amounts of UV ( $\lambda \leq 380$  nm, UVA intensity = 0.03 mW/cm<sup>2</sup>, UVB intensity = 0.015 mW/cm<sup>2</sup>, and UVC intensity = 0.006 mW/cm<sup>2</sup>), to confirm that natural sphalerite is a true VLD photocatalyst and the disinfection of *E. coli* K-12 is not due to UV photocatalysis, a sodium nitrite filter is placed between the light source and the flask to block all UV emission to ensure that the observed natural sphalerite disinfection performance is only due to VL photocatalysis. When the liquid filter was used, the intensity of VL decreased to 2.7 mW/cm<sup>2</sup> and no measurable UV intensity was detected. Under such conditions, total inactivation was achieved with 8 h of VL irradiation (Figure 1), which confirms that the observed bactericidal effect of natural sphalerite is not due to UV photocatalysis, and that natural sphalerite is a true VLD photocatalyst.

S-doping TiO<sub>2</sub><sup>17</sup> and Ag-coating TiO<sub>2</sub><sup>18</sup> are common synthetic VLD photocatalysts. Although these synthetic photocatalysts show high photocatalytic efficiency (1 h) under VL, only small amounts can be synthesized and these semiconductor modifications involve complicated techniques and are thus costly. In contrast, natural sphalerite occurs in large quantities in some zinc mines and is easily obtained making it much less costly than synthetic photocatalysts. More importantly, the most common VL sources for synthetic photocatalysts are Xenon lamp and halogen lamp, which have a high light intensity. However, these light sources cannot be widely used in wastewater treatment because of their high cost and high energy consumption. In this study, the fluorescent tubes are selected as the VL source because of their low cost and wide use in household lighting. Cheap and abundant natural photocatalysts coupled with 24 h opened fluorescent tubes are more promising

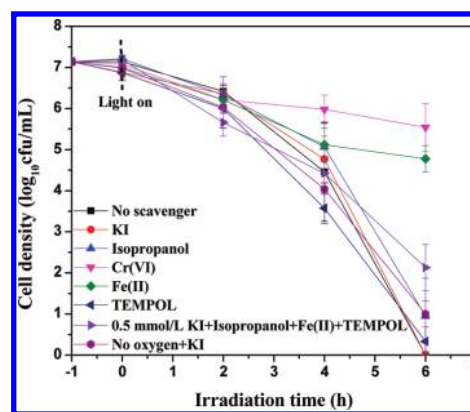


**Figure 2.** Disinfection efficiency of *E. coli* K-12 by the natural sphalerite with different scavengers (5 mmol/L KI, 0.5 mmol/L isopropanol, 0.05 mmol/L Cr(VI), 0.1 mmol/L Fe(II)-EDTA, 2 mmol/L TEMPOL) under VL irradiation.

than artificial photocatalysts for the photocatalytic disinfection of bacterial cells.

**3.2. Photocatalytic Disinfection Mechanism.** Photocatalysis is known to produce several reactive species ( $\cdot\text{OH}$ ,  $\text{H}_2\text{O}_2$ ,  $\cdot\text{O}_2^-$ ,  $\text{h}^+$ , and  $\text{e}^-$ ) that are potentially involved in the disinfection of bacterial cells. To determine which reactive species were involved in the photocatalytic disinfection process, different scavengers were used to remove the reactive species (Figure 2). The control experiments showed that the addition of these scavengers did not result in any toxic effect to *E. coli* K-12 within 6 h (Figure S4 of the Supporting Information). Without the addition of a scavenger, the complete disinfection of *E. coli* K-12 was achieved in a 6 h treatment. When Fe(II) ( $\text{H}_2\text{O}_2$  scavenger) was added, the cell density was reduced to  $1 \times 10^5$  cfu/mL without  $\text{H}_2\text{O}_2$  (Figure 2) indicating that  $\text{H}_2\text{O}_2$  is strongly involved in photocatalytic disinfection. In the presence of Cr(VI) ( $\text{e}^-$  scavenger), the cell density only decreased to  $5 \times 10^5$  cfu/mL (Figure 2), which suggests that  $\text{e}^-$  also play an important role in the disinfection process. In addition, the inhibitory effect of Cr(VI) did not only remove  $\text{e}^-$  but also prevented parts of  $\text{H}_2\text{O}_2$  formation by reduction of  $\text{O}_2$  by conduction band  $\text{e}^-$ , so the inactivation efficiency of *E. coli* K-12 in the presence of Cr(VI) was slightly lower than adding Fe(II). In the presence of isopropanol (diffusing  $\cdot\text{OH}$  scavenger), or TEMPOL ( $\cdot\text{O}_2^-$  scavenger), the level of the bactericidal effect did not change much compared with no scavenger (Figure 2) indicating that diffusing  $\cdot\text{OH}$  and  $\cdot\text{O}_2^-$  are not strongly involved in photocatalytic disinfection in this system. The result of adding KI ( $\text{h}^+$  and  $\cdot\text{OH}_s$  scavenger) was also similar to that of no scavenger (Figure 2), which suggests that  $\text{h}^+$  and  $\cdot\text{OH}_s$  are not involved in the disinfection. However, there is a worry that the possibly forming iodine species ( $\text{I}_2$ ) from KI oxidation also caused disinfection. Our experimental results showed that the level of  $\text{I}_2$  produced in the photocatalytic system was so low that below the detection limit of the iodine-starch assay (10  $\mu\text{g/L}$ )<sup>19</sup> and even 10  $\mu\text{g/L}$  of  $\text{I}_2$  was nontoxic to *E. coli*.<sup>20</sup> Therefore, we can exclude the contribution of  $\text{I}_2$  to the bacterial inactivation when using KI as the scavenger.

To further clarify whether  $\text{e}^-$  play an important role in photocatalytic disinfection, quadruple scavengers – KI, isopropanol, Fe(II), and TEMPOL – were employed to remove the  $\text{h}^+$ ,  $\cdot\text{OH}_s$ , diffusing  $\cdot\text{OH}$  in the bulk,  $\text{H}_2\text{O}_2$ , and  $\cdot\text{O}_2^-$  simultaneously (Figure 2), so that only  $\text{e}^-$  were left in the disinfection

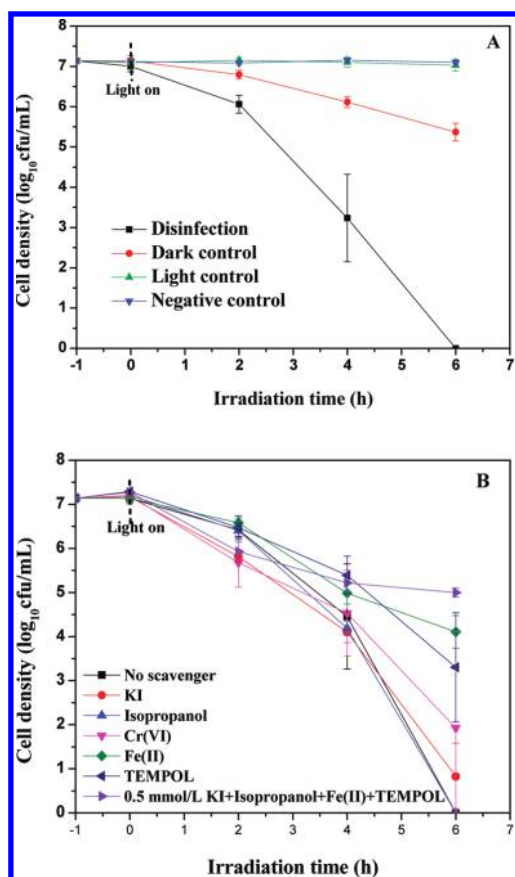


**Figure 3.** Photocatalytic disinfection of *E. coli* K-12 ( $1.5 \times 10^7$  cfu/mL) in the partition system. The bacterial cells are inside a semipermeable packaged container and outside of the membrane is the natural sphalerite suspension (1.00 g/L) under VL irradiation. (A) without scavenger, and (B) with different scavengers.

system. Interestingly, the presence of  $e^-$  resulted in a 5-log decrease in cell density after 6 h of treatment (Figure 2), which indicates that  $e^-$  are powerful reactive species for disinfecting *E. coli* K-12. This is probably due to the positioning of the conduction band of natural sphalerite at a much more negative potential ( $-1.4$  V vs SCE),<sup>21</sup> which give  $e^-$  the energy to inactivate bacteria. In addition, KI in the quadruple scavengers can remove  $h^+$  and prevent parts of  $e^-/h^+$  recombination, so that more  $e^-$  were available for disinfection than that of only adding Fe(II). Thus, the inactivation efficiency of *E. coli* K-12 in the presence of Fe(II) was lower than that with quadruple scavengers.

To further confirm the role of  $e^-$ , the photocatalytic disinfection of *E. coli* K-12 was conducted under anaerobic conditions (the reactor was sealed after 30 min of purging with Ar gas to eliminate  $O_2$ ) in the presence of  $h^+$  scavenger (KI) (Figure 2). In this system, no oxidative radicals were found either on the conduction band or on the valence band, and only  $e^-$  were involved in the disinfection. The result showed that the disinfection efficiency was higher under anaerobic than under aerobic condition, which further confirms the involvement of  $e^-$  in photocatalytic disinfection by natural sphalerite under VL irradiation.

To further determine the role of  $H_2O_2$  in disinfection, we conducted a photocatalytic disinfection of *E. coli* K-12 using a

partition system.<sup>9–11</sup> As shown in Figure S3 of the Supporting Information, the *E. coli* K-12 suspension was injected into a semipermeable membrane container and the natural sphalerite suspension was dispersed outside of the container. The molecular weight cutoff (MWCO) of the semipermeable membrane was 12 000–14 000 Da, which only allowed smaller molecules such as diffusing  $\cdot OH$  and  $H_2O_2$  to freely enter. The larger targets, such as natural sphalerite (which ranges in size from several nm to  $10 \mu m$ ) and *E. coli* K-12 (which has a molecular weight of about  $2.6 \times 10^6$  daltons) cannot pass through the membrane. Part A of Figure 3 showed the disinfection efficiency of *E. coli* K-12 inside the membrane container when the outside system was placed under different conditions. For the light and negative controls, the bacterial population showed no change after 6 h treatment, which indicates no toxic effect of light or the membrane on the cells. In the presence of natural sphalerite without light irradiation (dark control), only a 1.7-log reduction of *E. coli* K-12 was observed (part A of Figure 3), which was probably due to adsorption between the membrane and the cells of *E. coli* K-12. Interestingly, the complete inactivation of *E. coli* K-12 was observed after 6 h of treatment when the outer system was the natural sphalerite suspension irradiated by VL (part A of Figure 3). As mentioned previously, the natural sphalerite and *E. coli* K-12 were separated by a semipermeable membrane. This means the reactive species on the natural sphalerite surface, such as  $e^-$ ,  $h^+$ ,  $\cdot O_2^-$ , and  $\cdot OH$ s, should not have been involved in the disinfection in the partition system, and only diffusing reactive species, such as diffusing  $\cdot OH$  and  $H_2O_2$ , could pass through the membrane to inactivate *E. coli* K-12 inside the membrane container.

To find out which diffusing reactive species ( $\cdot OH$ ,  $H_2O_2$  or both) are involved in the disinfection process in the partition system, different scavengers were added into the outside of the membrane container to remove the respective reactive species. As shown in Figure S5 of the Supporting Information, the dark control showed an approximately 1.5-log reduction in disinfection, which was similar to the results for the dark control with no scavenger in the partition system (part A of Figure 3) and indicates that none of the scavengers are toxic to the cells. The addition of KI ( $h^+$  and  $\cdot OH$ s scavenger) (part B of Figure 3) did not change the level of bactericidal performance from that, when no scavenger was involved, which demonstrates that reactive species bound to the surface of the photocatalyst are not involved in the partition system or in the slurry system. When isopropanol (scavenger for diffusing  $\cdot OH$ ) was added, no obvious decrease in photocatalytic disinfection efficiency was observed compared with no scavenger (part B of Figure 3), which suggests that diffusing  $\cdot OH$  is also not involved in the bactericidal effect in this partition system. In the presence of TEMPOL ( $\cdot O_2^-$  scavenger), there was about a 4-log reduction in cell density after 6 h of irradiation. This decrease in disinfection efficiency was probably not due to the disinfection effect of  $\cdot O_2^-$  but to the inhibition effect of  $H_2O_2$  produced because of the removal of  $\cdot O_2^-$  by the scavengers.

The addition of Fe(II), which was the scavenger for  $H_2O_2$ , suppressed the bactericidal effect (part B of Figure 3). This result is similar to that in the nonpartition system (Figure 2), which indicates that  $H_2O_2$  plays an important role in both the partition system and nonpartition system in the photocatalytic disinfection of *E. coli* K-12.

In the partition system (part B of Figure 3), there was about a 5-log reduction in cell density in the presence of Cr(VI)

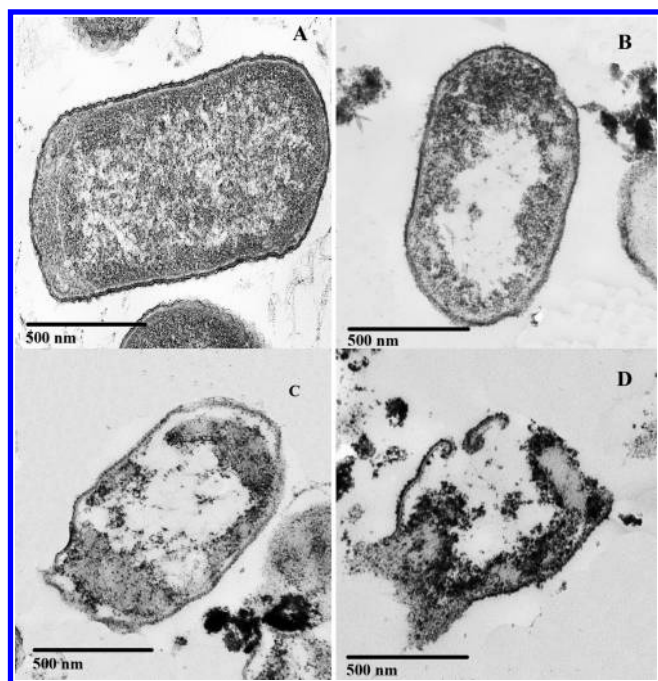


**Figure 4.** TEM images of *E. coli* K-12 photocatalytically treated with the natural sphalerite under VL irradiation adding quadruple scavengers (KI, isopropanol, Fe(II) and TEMPOL). (A) 0 h, (B) 6 h, (C) 12 h, and (D) 30 h.

( $e^-$  scavenger) after 6 h of irradiation, which suggests that  $e^-$  are not strongly involved in the disinfection in this system. In the nonpartition system (Figure 2), there was a slight decrease in cell density after the removal of  $e^-$  by adding Cr(VI) due to the important disinfecting role of  $e^-$ . In the partition system, the cell density was greatly reduced after adding Cr(VI) because of the lack of disinfection effect of  $e^-$ . We also added quadruple scavengers (KI, isopropanol, Fe(II), and TEMPOL) simultaneously to study the role of  $e^-$  in the partition system. The results showed that cell density decreased by 2-log (part B of Figure 3) and was similar to that of the dark control (Figure S5 of the Supporting Information), which indicates that  $e^-$  are probably not involved in disinfection in the partition system. In this system, the separation effected by the semipermeable membrane means that *E. coli* K-12 cannot come into direct contact with the surface of the natural sphalerite, so the  $e^-$  on the surface cannot display the bactericidal effect, and only  $H_2O_2$  diffuses through the membrane to inactivate the *E. coli* K-12 inside the membrane container. In the nonpartition system, because *E. coli* K-12 both contacts the surface and also reacts with the natural sphalerite solution, both  $e^-$  and  $H_2O_2$  are likely to be strongly involved in photocatalytic disinfection. The similar inactivation efficiency of *E. coli* K-12 in the nonpartition and partition systems may be due to the coworkers of conduction band  $e^-$  and  $H_2O_2$ , the latter of which was possibly produced by the reaction of conduction band  $e^-$  with dissolved  $O_2$ . In the nonpartition system, both conduction band  $e^-$  and the formed  $H_2O_2$  could react with bacterial cells, although the conduction band  $e^-$  was previously demonstrated by us to play a leading role in bacterial disinfection. By comparison, in the partition system, because there is not a direct contact between the conduction band  $e^-$  and the bacterial cells, most  $e^-$  are available for the production of  $H_2O_2$  before they contacted the bacteria. So the bacterial disinfection was mainly

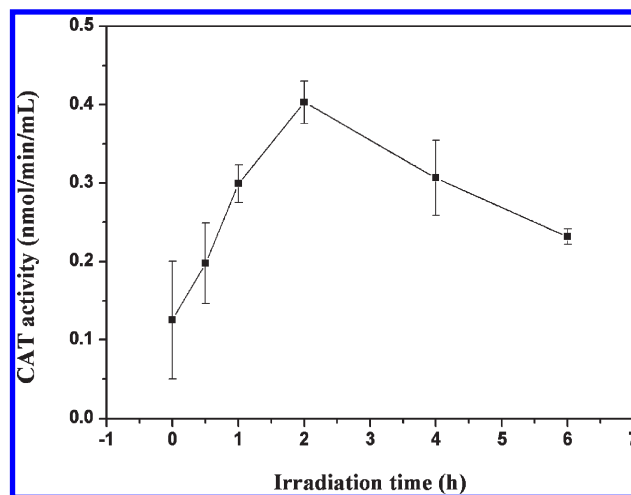


**Figure 5.** Induction of CAT activity under photocatalytic disinfection of *E. coli* K-12 by the natural sphalerite under VL irradiation.

contributed by the generated  $H_2O_2$ . Thus, the bactericidal effects in the nonpartition and partition systems can be similar because all of the bactericidal reactants were originated from the conduction band  $e^-$ .

**3.3. Transmission Electron Microscopy.** To further confirm the destruction process of *E. coli* K-12 by  $e^-$  or  $H_2O_2$  produced by natural sphalerite irradiated by VL, the cell morphology of *E. coli* K-12 was studied by TEM. Figure 4 shows the  $e^-$  disinfection effect after the addition of quadruple-scavengers (KI, isopropanol, Fe(II), and TEMPOL) at different stages of photocatalytic disinfection. In the initial stage of disinfection, *E. coli* K-12 exhibited an intact cell structure and an obvious cell wall (part A of Figure 4). After 6 h irradiation treatment (part B of Figure 4), an electron translucent region appeared at the center of the cell indicating that the outer membrane of the cell was damaged and thus a leakage of the interior components occurred. After 12 h treatment (part C of Figure 4), the cell had lost most of its interior components and the cell wall was partially destroyed, which suggested that the attack by  $e^-$  of the bacteria started from the outer membrane and then progressed to the cell wall. Eventually, as the irradiation time was extended to 30 h (part D of Figure 4), the cell became increasingly translucent and the cell wall was largely destroyed, indicating the complete destruction of *E. coli* K-12. Surprisingly, the  $e^-$  effect was similar to the effect of  $H_2O_2$  in the partition system (Figure S6 of the Supporting Information). Thus, one can speculate that  $e^-$  may react with a substrate/compound (X) to produce oxidative radical ( $\cdot X$ ). This substrate/compound (X) can be in the solution outside of the bacterial cell or inside of the bacterial cell. At present, we only know that  $e^-$  produced by natural sphalerite play an important role in disinfection, but the details of the mechanism of inactivation by  $e^-$  remain unknown. However, further investigation is needed to explain why  $e^-$  induced bacterial cell damage is similar to damage induced by reactive oxidative species (ROSs).

**3.4. Bacterial Catalase Activity.** To further confirm the role of  $H_2O_2$ , we also studied the effect of catalase (CAT) (Figure 5), a well-known antioxidant enzyme that defends against oxidative stress from the environment, on VLD photocatalytic disinfection. CAT catalyzes the decomposition of  $H_2O_2$  to water and oxygen. As CAT is an enzyme that protects bacteria from  $H_2O_2$ , a

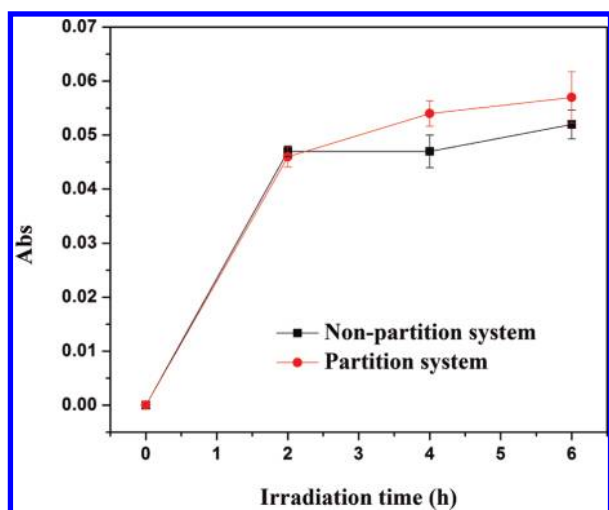


**Figure 6.** Absorption intensity (551 nm) of DPD/POD reagent after reaction with  $\text{H}_2\text{O}_2$  against illumination time in the nonpartition and partition systems.

higher CAT activity implies that bacteria are encountering a more significant  $\text{H}_2\text{O}_2$  attack and can better defend against  $\text{H}_2\text{O}_2$  attack from photocatalytic disinfection. As shown in Figure 5, in the initial 2 h, CAT activity increased rapidly with time, which indicates there is a large amount of  $\text{H}_2\text{O}_2$  attacking the bacteria at the beginning of the photocatalytic disinfection, with the bacterial defense system displaying a higher CAT activity to protect the bacteria. This observation matches with the results of Figure 1 that showed that the disinfection efficiency increased very slowly in the initial 2 h because antioxidant enzyme protected the *E. coli* K-12. After 2 h, CAT activity gradually decreased as the disinfection process progressed (Figure 5). This result can be explained by the rapid increase in disinfection efficiency after 2 h (Figure 1). Because the amount of  $\text{H}_2\text{O}_2$  produced by the natural sphalerite exceeded the protection ability of the defense system, *E. coli* K-12 was severely damaged, and the CAT activity decreased again. This evidence further indirectly indicates that  $\text{H}_2\text{O}_2$  plays an important role in photocatalytic disinfection.

**3.5. Analysis of  $\text{H}_2\text{O}_2$ .** The  $\text{H}_2\text{O}_2$  produced by the natural sphalerite was further determined by a photometric method using peroxidase (POD).<sup>16</sup> Figure 6 shows the absorbance (at 551 nm) of  $\text{H}_2\text{O}_2$  against irradiation time in the nonpartition and partition systems and clearly demonstrates that  $\text{H}_2\text{O}_2$  was accumulated in both systems. Although the concentration of  $\text{H}_2\text{O}_2$  in both systems was only on the level of several micrometers;<sup>16</sup> however, in photocatalytic disinfection,  $\text{H}_2\text{O}_2$  is continuously produced and consumed dynamically, which means the total amount of  $\text{H}_2\text{O}_2$  produced in the system is much more than actually measured value. Thus, we can confirm that the contribution of  $\text{H}_2\text{O}_2$  to disinfection is present in both systems.

Several previous studies have focused on the bactericidal effects of ROSs. Some have suggested that  $\cdot\text{OH}$  is the primary attacking agent in the photocatalytic bactericidal effect due to its powerful oxidative ability.<sup>11,22,23</sup> Other studies have suggested that the main bactericidal agent in photocatalytic disinfection is not  $\cdot\text{OH}$  but  $\text{H}_2\text{O}_2$ , because  $\cdot\text{OH}$  has a very short lifetime,<sup>24,25</sup> whereas  $\text{H}_2\text{O}_2$  can diffuse through the cell membrane and produce a long-range bactericidal effect.<sup>26,27</sup> In the natural

sphalerite–VL system, we posit that  $\cdot\text{OH}$  may not be the bactericidal agent due to its short lifetime and that instead  $\text{H}_2\text{O}_2$ , because of its long lifetime and ability to diffuse into the bacteria, is the main agent in the disinfection process.

## ■ ASSOCIATED CONTENT

**S Supporting Information.** Setup of nonpartition system and partition system, the optimization of photocatalyst, the dark and light control of scavenger effect in nonpartition and partition system, and TEM images of bactericidal effect of  $\text{H}_2\text{O}_2$ . This material is available free of charge via the Internet at <http://pubs.acs.org>.

## ■ AUTHOR INFORMATION

### Corresponding Author

\*Phone: +852-2609 6383; Fax: +852 2693 5767; E-mail: [pkwong@cuhk.edu.hk](mailto:pkwong@cuhk.edu.hk).

## ■ ACKNOWLEDGMENT

The project was supported by research grants from the Research Grants Council of the Hong Kong SAR Government to P.K. Wong (Grant No. GRF 477610), the National Basic Research Program of China to A.H. Lu (Program No. 2007CB815602), and the National Natural Science Foundation of China to Yan Li (Grant No. 40902016).

## ■ REFERENCES

- (1) Hoffmann, M. R.; Martin, S. T.; Choi, W.; Bahnemann, D. W. Environmental applications of semiconductor photocatalysis. *Chem. Rev.* **1995**, *95*, 69–96.
- (2) Matsunaga, T.; Tomodam, R.; Nakajima, T.; Wake, H. Photoelectrochemical sterilization of microbial cells by semiconductor powders. *FEMS Microbiol. Lett.* **1985**, *29*, 211–214.
- (3) Depero, L. E. Coordination geometry and catalytic activity of vanadium on  $\text{TiO}_2$  surfaces. *J. Solid State Chem.* **1993**, *103*, 528–532.
- (4) Leung, T. Y.; Chan, C. Y.; Hu, C.; Yu, J. C.; Wong, P. K. Photocatalytic disinfection of marine bacteria using fluorescent light. *Water Res.* **2008**, *42*, 4827–4837.
- (5) Li, Y.; Lu, A. H.; Wang, C. Q. Semiconducting mineralogical characteristics of natural sphalerite gestating visible-light photocatalysis. *Acta Geol. Sin* **2009**, *83*, 633–639.
- (6) Li, Y.; Lu, A. H.; Wang, C. Q. Photocatalytic reduction of  $\text{Cr(VI)}$  by natural sphalerite suspensions under visible light irradiation. *Acta Geol. Sin* **2006**, *80*, 267–272.
- (7) Li, Y.; Lu, A. H.; Wang, C. Q.; Wu, X. L. Characterization of natural sphalerite as a novel visible-light-driven photocatalyst. *Solar Energy Mater. Solar Cells* **2008**, *92*, 953–959.
- (8) Li, Y.; Lu, A. H.; Jin, S.; Wang, C. Q. Photo-reductive decolorization of an azo dye by natural sphalerite: case study of a new type of visible light-sensitized photocatalyst. *J. Hazard. Mater.* **2009**, *170*, 479–486.
- (9) Kikuchi, Y.; Sunada, K.; Iyoda, T.; Hashimoto, K.; Fujishima, A. Photocatalytic bactericidal effect of  $\text{TiO}_2$  thin films: dynamic view of the active oxygen species responsible for the effect. *J. Photochem. Photobiol. A: Chem.* **1997**, *106*, 51–56.
- (10) Zhang, L. S.; Wong, K. H.; Zhang, D. Q.; Hu, C.; Yu, J. C.; Chan, C. Y.; Wong, P. K.  $\text{Zn:In(OH)}_y\text{S}_z$  solid solution nanoplates: synthesis, characterization, and photocatalytic mechanism. *Environ. Sci. Technol.* **2009**, *43*, 7883–7888.
- (11) Zhang, L. S.; Wong, K. H.; Yip, H. Y.; Hu, C.; Yu, J. C.; Chan, C. Y.; Wong, P. K. Effective photocatalytic disinfection of *E. coli* K-12 using  $\text{AgBr-Ag-Bi}_2\text{WO}_6$  nanojunction system irradiated by visible

light: the role of diffusing hydroxyl radicals. *Environ. Sci. Technol.* **2010**, *44*, 1392–1398.

(12) Chen, Y. X.; Yang, S. Y.; Wang, K.; Lou, L. P. Role of primary active species and TiO<sub>2</sub> surface characteristic in UV-illuminated photo-degradation of Acid Orange 7. *J. Photochem. Photobiol. A: Chem.* **2005**, *172*, 47–54.

(13) Khodja, A. A.; Boulkamh, A.; Richard, C. Phototransformation of metobromuron in the presence of TiO<sub>2</sub>. *Appl. Catal. B: Environ.* **2005**, *59*, 147–154.

(14) Lejeune, D.; Hasanuzzaman, M.; Pitcock, A.; Francis, J.; Sehgal, I. The superoxide scavenger TEMPOL induces urokinase receptor (uPAR) expression in human prostate cancer cells. *Mol. Cancer* **2006**, *5*, 21–26.

(15) Cayman Chemical Company, *Protocol for Catalase Assay*; Ann Arbor: MI, USA, 2009.

(16) Bader, H.; Sturzenegger, V.; Hoigné, J. Photometric method for the determination of low concentrations of hydrogen peroxide by the peroxidase catalyzed oxidation of N, N-diethyl-p-phenylenediamine (DPD). *Water Res.* **1988**, *22*, 1109–1115.

(17) Yu, J. C.; Ho, W. K.; Yu, J. G.; Yip, H. Y.; Wong, P. K.; Zhao, J. C. Efficient visible-light-induced photocatalytic disinfection on sulfur-doped nanocrystalline titania. *Environ. Sci. Technol.* **2005**, *39*, 1175–1179.

(18) Zhang, L. Z.; Yu, J. C.; Yip, H. Y.; Li, Q.; Kwong, K. W.; Xu, A. W.; Wong, P. K. Ambient light reduction strategy to synthesize silver nanoparticles and silver-coated TiO<sub>2</sub> with enhanced photocatalytic and bactericidal activities. *Langmuir* **2003**, *19*, 10372–10380.

(19) Tsunogai, S. Determination of iodine in sea water by an improved Sugawara's method. *Anal. Chim. Acta* **1971**, *55*, 444–447.

(20) Backer, H.; Hollowell, J. Use of iodine for water disinfection: iodine toxicity and maximum recommended dose. *Environ. Health Perspect.* **2000**, *108*, 679–684.

(21) Zang, L.; Liu, C. Y.; Ren, X. M. Photochemistry of semiconductor particles 3. Effects of surface charge on reduction rate of methyl orange photosensitized by ZnS sols. *J. Photochem. Photobiol. A: Chem.* **1995**, *85*, 239–245.

(22) Watts, R. J.; Kong, S.; Orr, M. P.; Miller, G. C.; Henry, B. E. Photocatalytic inactivation of coliform bacteria and viruses in secondary wastewater effluent. *Water Res.* **1995**, *29*, 95–100.

(23) Cho, M.; Chung, H.; Choi, W.; Yoon, J. Different inactivation behaviors of MS-2 phage and *Escherichia coli* in TiO<sub>2</sub> photocatalytic disinfection. *Appl. Environ. Microbiol.* **2005**, *71*, 270–275.

(24) Blake, D. M.; Maness, P. C.; Huang, Z.; Wolfrum, E. J.; Huang, J.; Jacoby, W. A. Application of the photocatalytic chemistry of titanium dioxide to disinfection and the killing of cancer cells. *Sep. Purif. Methods* **1999**, *28*, 1–50.

(25) Strul, G.; Frimer, A. A.; Weiner, L. Spin-trapping study of free radical penetration into liposomal membranes. *J. Chem. Soc., Perkin Trans.* **1993**, *2*, 2057–2059.

(26) Bors, W.; Michel, C.; Saran, M. On the nature of biochemically generated hydroxyl radicals. *Eur. J. Biochem.* **1979**, *95*, 621–627.

(27) Rincón, A. G.; Pulgarin, C. Effect of pH, inorganic ions, organic matter and H<sub>2</sub>O<sub>2</sub> on *E-coli* K12 photocatalytic inactivation by TiO<sub>2</sub> - Implications in solar water disinfection. *Appl. Catal. B: Environ.* **2004**, *51*, 283–302.

1 **Supporting information**

2  
3 **Naturally occurring sphalerite as a novel cost-effective photocatalyst**  
4 **for bacterial disinfection under visible light**

5  
6 Yanmin Chen,<sup>†</sup> Anhuai Lu,<sup>§</sup> Yan Li,<sup>§</sup> Lisha Zhang,<sup>†</sup> Ho Yin Yip,<sup>†</sup> Huijun Zhao,<sup>‡</sup>

7 Taicheng An,<sup>#</sup> and Po-Keung Wong<sup>\*,†</sup>

8  
9 <sup>†</sup>School of Life Sciences, The Chinese University of Hong Kong, Shatin, NT, Hong  
10 Kong SAR, China

11 <sup>§</sup>The Key Laboratory of Orogenic Belts and Crustal Evolution, School of Earth and  
12 Space Sciences, Peking University, Beijing 100871, China

13 <sup>‡</sup>Centre for Clean Environment and Energy, and Griffith School of Environment,  
14 Gold Coast Campus, Griffith University, Queensland 4222, Australia

15 <sup>#</sup>State Key Laboratory of Organic Geochemistry, Guangzhou Institute of  
16 Geochemistry, Chinese Academy of Sciences, Guangzhou 510640, China

17  
18  
19  
20  
21 

---

  
\*Corresponding author: Tel: +852-2609 6383, Fax: +852 2693 5767;

22 E-mail: [pkwong@cuhk.edu.hk](mailto:pkwong@cuhk.edu.hk)

23  
24  
25 Ref: Supporting Information-240511.doc

26 **CONTENTS:**

27

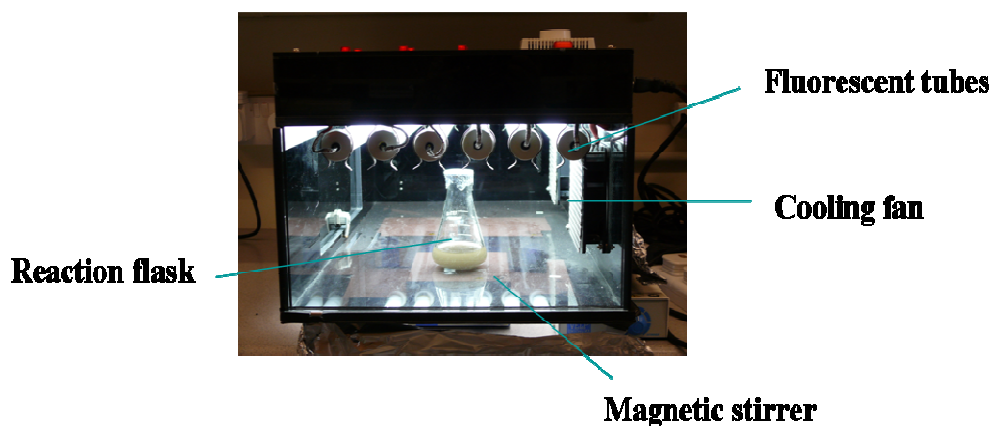
- 28 1. A photo of the photoreactor and light source.
- 29 2. Optimize the concentration of the natural sphalerite for the photocatalytic  
30 disinfection.
- 31 3. Illustration of partition system setup.
- 32 4. Dark control and Light control in presence of different scavengers in non-partition  
33 system.
- 34 5. Dark control and Light control in presence of different scavengers in partition  
35 system.
- 36 6. TEM images of *E. coli* K-12 photocatalytically treated with the natural sphalerite  
37 under VL irradiation in partition system.

38

39 **Number of pages: 7**

40 **Number of Figures: 6**

41 1. A photo of the photoreactor and light source.

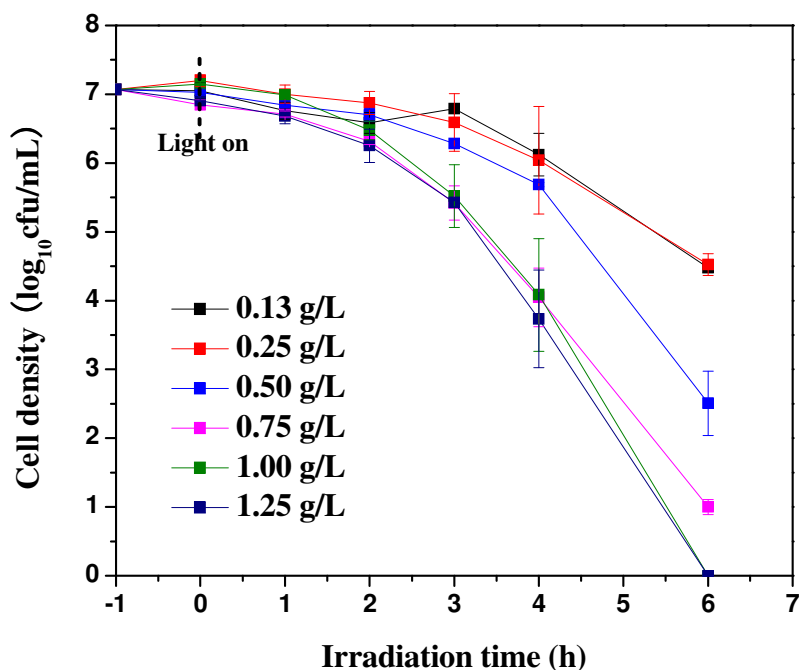


42

43 Figure S1. A photo of the photocatalytic disinfection unit under fluorescent tubes  
44 irradiation

45

46 2. Optimize the concentration of the natural sphalerite for the photocatalytic  
47 disinfection.

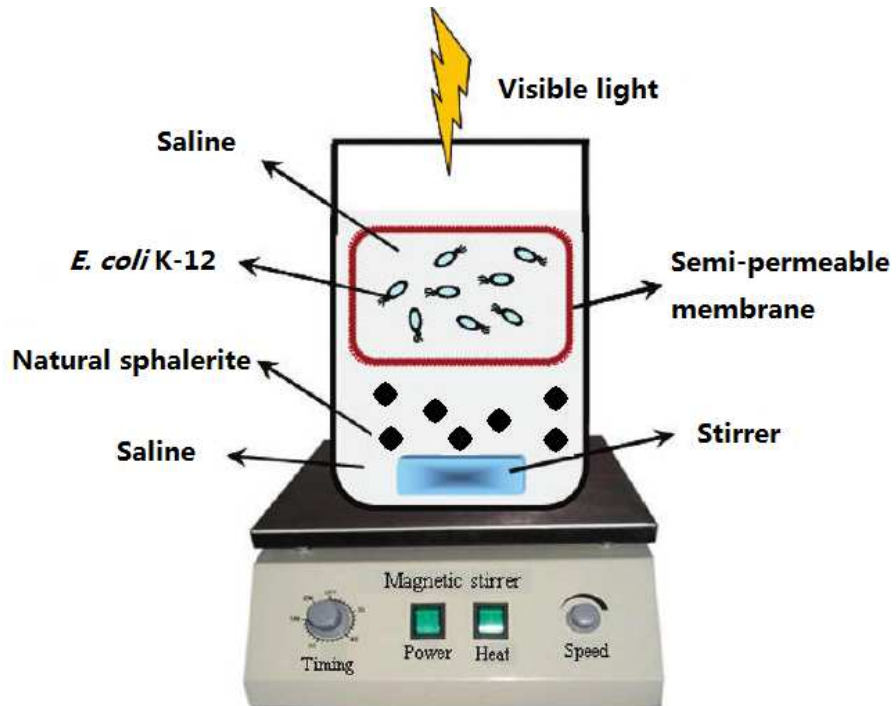


48

49 Figure S2. Disinfection efficiency of *E. coli* K-12 ( $1.5 \times 10^7$  cfu/mL) at the different  
50 concentration of the natural sphalerite under VL irradiation.

51 **3. Illustration of partition system setup.**

52

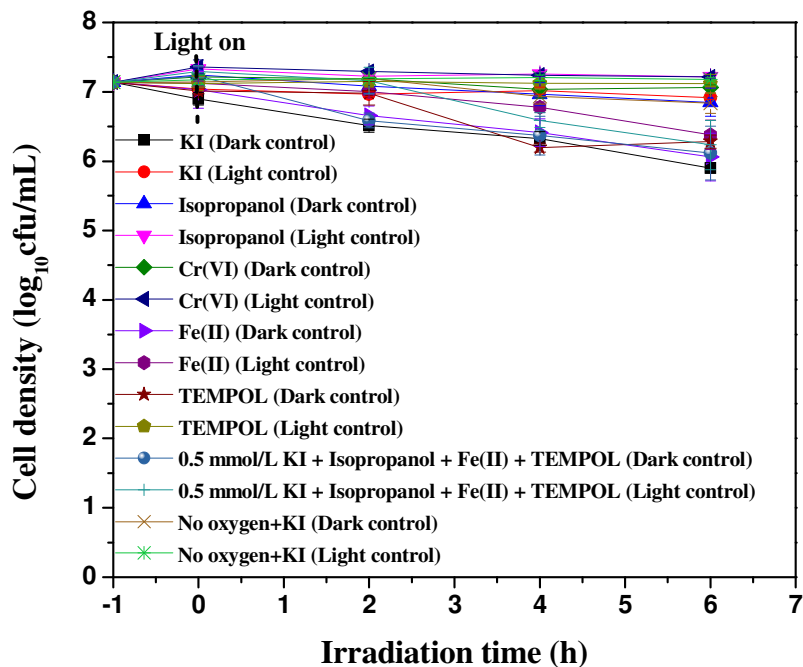


53

54

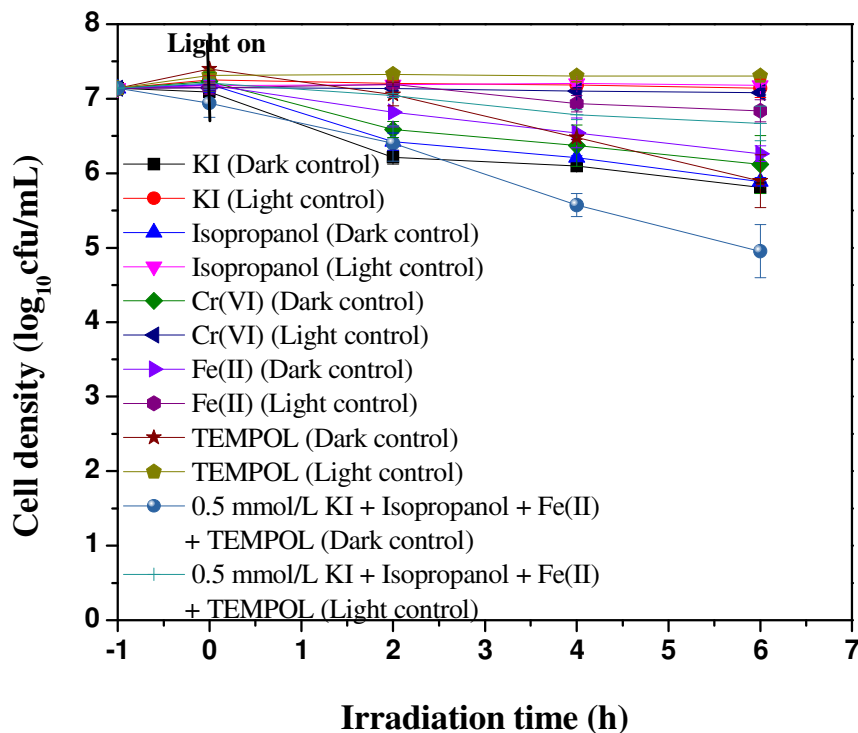
55 Figure S3. Schematic illustration of partition system setup used in the photocatalytic  
56 disinfection of *E. coli* K-12 with the natural sphalerite under VL irradiation.

57 **4. Dark control and Light control in presence of different scavengers in**  
 58 **non-partition system.**



59  
 60 Figure S4. Disinfection efficiency of *E. coli* K-12 by the natural sphalerite under VL  
 61 irradiation with different scavengers in dark control (50 mg natural sphalerite without  
 62 visible light irradiation) and light control (visible light irradiation without the natural  
 63 sphalerite) (5 mmol/L KI, 0.5 mmol/L Isopropanol, 0.05 mmol/L Cr(VI), 0.1 mmol/L  
 64 Fe(II)-EDTA, 2 mmol/L TEMPOL).

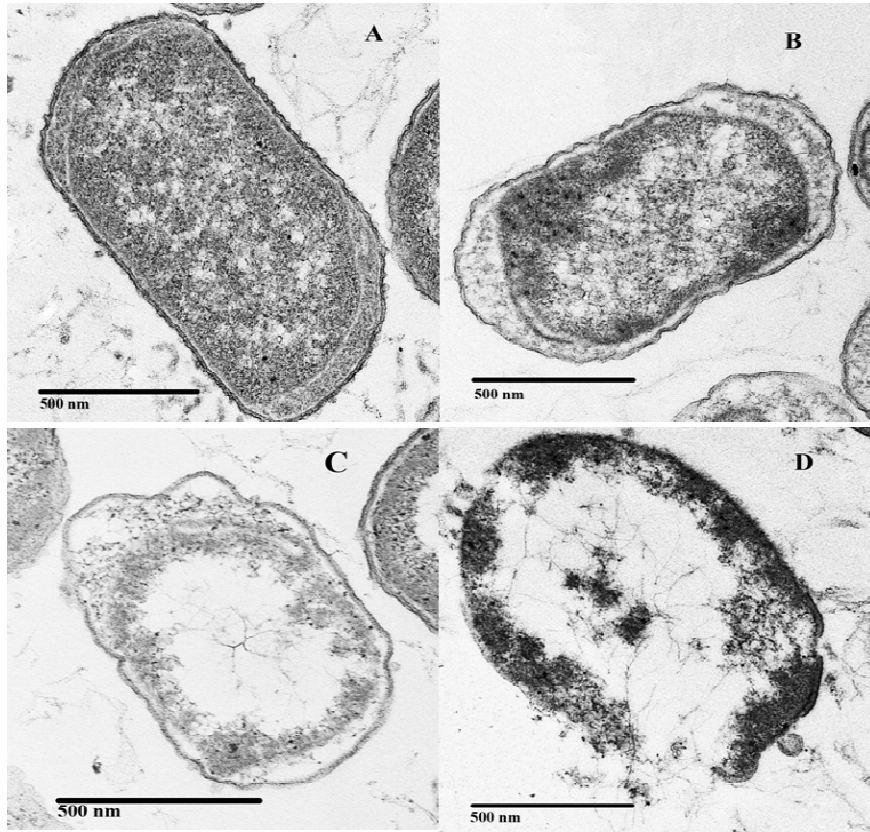
65 **5. Dark control and Light control in presence of different scavengers in**  
 66 **partition system.**



67  
 68 Figure S5. Photocatalytic disinfection of *E. coli* K-12 ( $1.5 \times 10^7$  cfu/mL) in the  
 69 partition system. The bacterial cells are inside a semi-permeable packaged container  
 70 and outside of the membrane is the natural sphalerite suspension (1.00 g/L) under VL  
 71 irradiation with different scavengers in dark control (50 mg natural sphalerite without  
 72 visible light irradiation) and light control (visible light irradiation without the natural  
 73 sphalerite) (5 mmol/L KI, 0.5 mmol/L Isopropanol, 0.05 mmol/L Cr(VI), 0.1 mmol/L  
 74 Fe(II)-EDTA, 2 mmol/L TEMPOL).

75 **6. TEM images of *E. coli* K-12 photocatalytically treated with the natural**  
76 **sphalerite under VL irradiation in partition system.**

77



78

79

80 Figure S6. TEM images of *E. coli* K-12 photocatalytically treated with the natural  
81 sphalerite under VL irradiation in the partition system (A) 0 h, (B) 6 h, (C) 12 h, and  
82 (D) 30 h.